IMPACT OF NON-RADIATIVE RECOMBINATIONS IN THIN FILM SOLAR CELLS WITH LIGHT-TRAPPING: AN ANALYTIC MODEL

A. Bozzola, P. Kowalczewski, M. Farina, and L.C. Andreani
University of Pavia, Italy
Via Bassi 6, 27100, Pavia, Italy

ABSTRACT: We propose an analytic electro-optical model for solar cells, and we apply it to investigate the interplay between non-radiative recombination and light trapping in crystalline silicon p-n junctions. We adopt a Lambertian scatterer as prototype for devices incorporating light trapping, and we take into account recombination both in the bulk and at interfaces by calculating analytic solutions of the transport equations. We show that solar cells with Lambertian light trapping and characteristic thickness of the order of a few tens of microns are the best choice in terms of conversion efficiency. By using our model, we quantify the optimal thickness depending on the material quality. Surface dynamics become a crucial factor when reducing the devices thickness and its importance is amplified in real devices where textures are used to implement light trapping, due to increased surface area. We estimate the maximum level of (effective) surface recombination which is required for thin-film cells to overcome the bulk ones, and to approach their realistic ultimate efficiency.

Keywords: Modeling, Light Trapping, Recombination

1 MOTIVATIONS OF THIS WORK

In the last years the topic of light trapping in silicon solar cells enlivened both the scientific and PV industrial communities with the common aim of developing thin and cheap devices, while preserving high conversion efficiency [1-4]. Although many progresses have been made in developing photonic structures that show excellent light trapping properties [5-10], the issue of realistic energy conversion efficiency has not been treated analytically in detail. This topic was first investigated during the '80s for the case of crystalline silicon (c-Si) p-n junction solar cells [11,12]. In these years it was shown that intrinsic recombination mechanisms such as radiative and Auger limit the ultimate efficiency to 29.8%, with an optimal thickness around 80 microns. Defects-mediated non-radiative recombination, however, was not included. Present day state-of-the-art devices [13] exhibit maximum efficiency around 25%, which is obtained using much thicker, high quality wafers (400 μm). Thus extrinsic recombination and light confinement are crucial factors to improve conversion efficiency. In particular, defects-mediated recombination at surfaces plays a central role in thin devices incorporating surface textures for light trapping. In fact, the surface to volume ratio is larger than in bulk cells, and the surface area may be significantly enhanced by the textures. A trade-off occurs, as light trapping comes at the expense of increased surface recombination: light trapping can improve the device performance only if good surface passivation is achieved.

At the end of the '90s M. A. Green tried to incorporate surface recombination and Lambertian light trapping in a single electro-optical model [14]. However, the model does not employ a surface recombination velocity, but rather the corresponding open-circuit voltage. This quantity is dependent on the device structure under consideration, and limits the applicability of the proposed model to other materials and cell's architectures. In addition, it was shown that as soon as surface recombination is introduced, the optimal cell thickness moves from 80 μm to the bulk regime, implying that thin-film devices are not competitive with bulk ones. It would be very useful to evaluate the interplay of surface recombination, increased surface area, and light trapping in a single model with a larger range of applicability.

In this work we propose an analytic electro-optical model which incorporates light trapping at the Lambertian limit [15] and non-radiative recombinations both in the bulk and at interfaces. The model is fully validated against numerical solutions of the drift-diffusion equations, obtaining a good agreement. We show that p-n junction c-Si solar cells with thickness around a few tens of microns are the best solution in terms of conversion efficiency, provided that (effective) surface recombination velocities are kept below a critical level, which is precisely quantified by the model. We estimate also the maximum (effective) surface recombination velocity which is needed for solar cells to approach their ultimate efficiency. We show that state-of-the-art technologies for surface texture and passivation have the potential to improve silicon solar cells efficiencies above present day's values for bulk devices.

2 THE STRUCTURES UNDER INVESTIGATION

The structures under investigation are sketched in Fig. 1. We consider planar cells and solar cells with ideal Lambertian light trapping. The total silicon thickness is denoted as *w*.

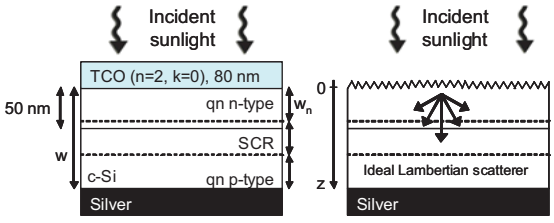

Fig. 1. Sketch of the solar cells structures under investigation: planar cells with single-layer AR coating (left), and with ideal Lambertian light trapping (right).

For planar devices we assume a single layer, transparent anti-reflection (AR) coating with thickness 80 nm and real part of the refractive index n=2. Textured solar cells have no reflection losses and have an ideal Lambertian front scattering layer [15]. The intensity of light scattered inside the active layer is proportional to $\cos\theta$, where θ denotes the angle with respect to the surface normal

(along z, see Fig. 1). In both cases we assume a semi-infinite silver back reflector. Optical data for c-Si and Ag are taken from Palik [16]. Electrical properties of the devices are analyzed in the framework of depletion region approximation for semiconductor p-n homojunctions [17-19]. We assume a central space charge region (SCR) across the junction plane, and two adiacent quasi-neutral (qn) regions. We denote the SCR width as w_{scr}, and the widths of the qn regions as w_n and w_p.

We assume a heavily doped (10^{19} cm^{-3}), 50 nm thick, n-type emitter, and a lightly doped (10^{16} cm^{-3}) p-type base. With the selected doping levels, the depletion approximations allows estimating the SCR width as w_{scr}=350 nm, which is almost totally located in the base region.

The total current flowing through the device is expressed as the sum of three contributions generated in the different regions of the cell. The external quantum efficiency is thus expressed as:

$$EQE(E) = EQE_n(E) + EQE_{scr}(E) + EQE_p(E), \quad (1)$$

and a similar subdivision holds for the dark current flowing under applied bias V:

$$J_{dark}(V) = J_{dark,n}(V) + J_{dark,scr}(V) + J_{dark,p}(V). \quad (2)$$

3 ANALYTIC ELECTRO-OPTICAL MODEL

The proposed analytic electro-optical model can be summarized in three steps:

I. Calculation of the carrier generation rate;
II. Solution of the diffusion equations for minority carriers generated in the qn regions, and calculation of EQE and J_{sc};
III. Solution of the diffusion equation in the dark, and calculation of the JV curve of the device.

The carrier generation rate $g(z,E)$ is calculated analytically using Poyting vector ($\boldsymbol{S}$) analysis. Denoting the incident Poyting vector amplitude as S_{0z}, g is given as:

$$g(z,E) = \left[-\frac{1}{S_{0z}} \frac{dS(z)}{dz} \right] \phi_{AM1.5}(E) , \quad (3)$$

where $\Phi_{AM1.5}(E)$ denotes the incident AM 1.5 photon flux. For planar cells, $\boldsymbol{S}$ is obtained directly from the electric field amplitudes, which are calculated within the device using a transfer matrix approach [20]. For cells with light trapping, $\boldsymbol{S}$ is expressed as the sum of two hemispherical contributions for upward and downward propagation along z [15]. According to Eq. (3), g writes as:

$$g(z,E) = \frac{\alpha_{lt}\left(R_b e^{-2\alpha_{lt}w} e^{\alpha_{lt}z} + e^{-\alpha_{lt}z}\right)}{1 - R_b e^{-2\alpha_{lt}w}\left(1 - 1/n_{Si}^2\right)} \phi_{AM1.5}(E) \quad (4)$$

Here α_{lt} denotes the effective absorption coefficient in presence of light path enhancement [21], R_b is the rear reflectance averaged over incidence angle and polarizations, and n_{Si} is the refractive index of of silicon.
In order to verify that Eq. (4) is a good approximation of where light is absorbed within a realistic device with light trapping, we compare with the carrier generation rate of a silicon cell with the same thickness and optimized front scattering roughness, which is calculated using Rigorous Coupled Wave Analysis (RCWA) [8]. The comparison between the two types of structures is shown in Fig. 2.

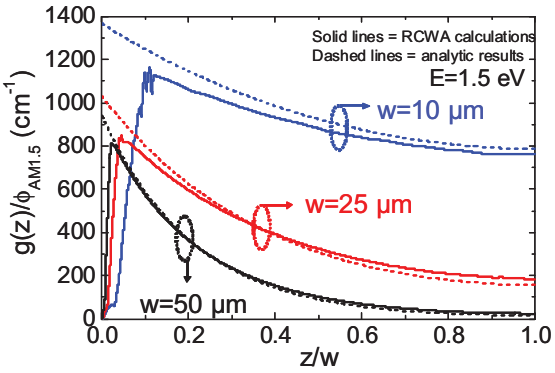

Fig. 2. Comparison between the carrier generation rate at E=1.5 eV (normalized to the incident photon flux) calculated using Eq. (4), and for silicon cell incorporating a rough silicon / dielectric interface calculated using RCWA.

As it can be seen, apart from small discrepancies which are due to reflection losses and incomplete light confinement, the agreement is very good. Eq. (2) is crucial to reduce the optical problem from 3D to 1D, and to get analytic solutions.

The total absorption for flat and textured solar cells with thickness w = 1 µm is shown in Fig. 3.

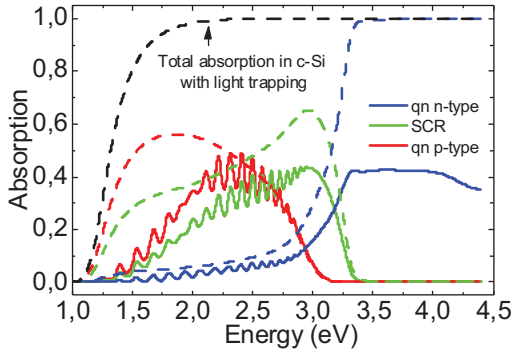

Fig. 3. Absorption within the SCR and qn regions of a planar solar cell (dashed lines), and of a cell with Lambertian light trapping. The thickness is w=1 µm. In the latter case, the total absorption in the silicon layer is also reported.

We report the absorption within the top (bottom) qn region with blue (red) lines, and the absorption within the SCR with green lines. As shown, Lambertian light trapping drastically improves absorption of low energy photons, with resulting increased photogenerated current.
The calculated carrier generation rates enter in the steady-state drift-diffusion equations for photogenerated excess minority carriers. We assume that the SCR is free of internal losses due to the built-in electric field [17-19]. For the n-type qn region, the diffusion equation for holes writes as:

$$\frac{d^2\Delta p}{dz^2} - \frac{\Delta p}{L_n^2} + \frac{g(z,E)}{D_n} = 0 \quad (5)$$

Here Δp denotes the excess holes concentration, L_n the diffusion length, and D_n the diffusion constant. A similar

equation holds for electrons in the p-type. In this work we assume D_n=2 cm^2/s and D_p=40 cm^2/s as representative values for c-Si [17]. Surface recombination enters in the boundary conditions:

$$D_n\left(\frac{d\Delta p}{dz}\right)_{z=0} = S_n \Delta p(z=0) \quad (6)$$

$$\Delta p(z=w_n) = 0 \quad (7)$$

For cells with light trapping, the increased surface area due to texturing leads to increased S compared to the flat case. In this case we define the surface area enhancement as K_{area}, and rewrite Eq. (6) as:

$$D_n\left(\frac{d\Delta p}{dz}\right)_{z=0} = K_{area} S_n \Delta p(z=0) \quad (8)$$

The Δp terms are calculated using the Lambertian carrier generation rate of Eq. (4), and the effective surface recombination velocity $S_{n,eff} = K_{area}S_n$ is introduced. Eq. (8) is fundamental to reduce also the transport problem from 3D to 1D, so that analytic solutions can be found easily.

The last step of modeling is the calculation of the dark current, following the depletion region approximation for semiconductor p-n junctions [17].
The total current density flowing through the cells is expressed as $J(V)=J_{sc}-J_{dark}(V)$, where we approximate the photogenerated current with the short-circuit current. The energy conversion efficiency is thus expressed as a function of the cell's main electrical parameters: $\eta=FF\times J_{sc}\times V_{oc}/P_{inc}$, where P_{inc} is the incident AM 1.5 power, 100 mW/cm^2.

4 EFFECTS OF THE SILICON THICKNESS AND OF THE BULK MATERIAL QUALITY

As the first step of our analysis, we checked the effects of the c-Si layer thickness for both planar and textured solar cells: results are reported in Fig. 4.

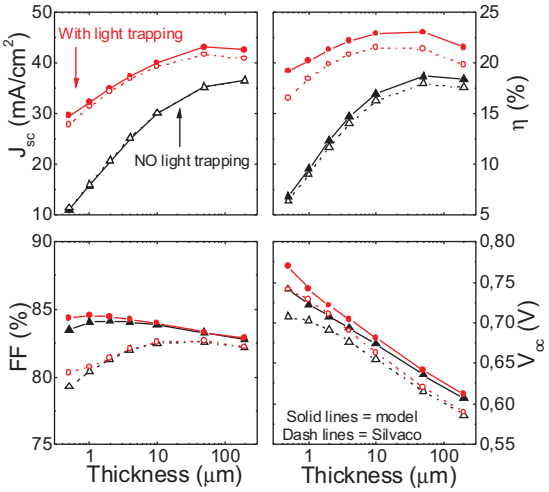

Fig. 4. Main electrical parameters for flat cells (black curves), and for cells with ideal Lambertian light trapping (red curves). Analytic results are reported with solid lines and closed symbols, while numerical results obtained with the Silvaco ATLAS software package are shown with dashed lines and open symbols.

For this case, we fix L_n=20 μm, L_p=200 μm, and we assume ideal surface passivation, S_n = S_p = 0 cm/s. As shown, J_{sc} and V_{oc} have opposite trends as functions of thickness. The former keeps increasing, and it is drastically improved when light trapping is incorporated. The latter, instead, decreases due to larger dark current in thicker devices.
These opposite trends determine a maximum in conversion efficiency. For planar cells, this is below 20% efficiency, and it is achieved using a silicon thickness in the range 50-100 μm. For cells with light trapping, maximum efficiency is above 23%, with the optimal thickness in the thin-film range, around 30 μm. We validate our model against numerical solutions of the transport equations obtained using the Silvaco ATLAS software package. Numerical results are reported with dashed lines and open symbols in Fig. 4. As evident, the agreement is good for the short-circuit current, while the model systematically overestimates V_{oc} and η by around 10%. This is in line with the model's approximations: (i) no recombination for excess carriers photogenerated in the SCR, and (ii) approximation of the photocurrent with the J_{sc}. Despite such small discrepancies, we note that all the trends are correctly reproduced.

The next step concerns the effects of bulk recombination, which determines the optimal cell thickness in presence of ideal surface passivation. Results are reported in Fig. 5, where we report the efficiency of solar cells with ideal Lambertian light trapping and perfect surface passivation, as a function of the minority carriers diffusion length (L_n=L_p), of the thickness w.

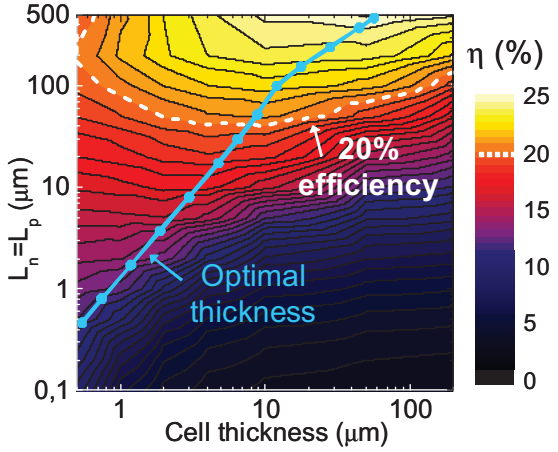

Fig. 5. Energy conversion efficiency for solar cells with ideal Lambertian light trapping and perfect surface passivation (S_n=S_p=0) as a function of the bulk quality (L_n=L_p) and cell thickness. The useful range with η exceeding 20% is reported within a dashed white line, while the optimal configurations lie along the blue solid line.

The optimal configurations lie along the blue solid line, and are characterized by an optimal thickness which is always below 80 μm. In particular, the optimal thickness is 5 to 10 times smaller than minority carriers' diffusion length. The requirement is more stringent than the one dictated by simple diffusion of photogenerated minority carriers ($w \leq L$). This is due to the V_{oc}, which favors thin cells over the bulk ones.
To compete with conventional wafer technology, thin-

film solar cells should reach high efficiency above 20%, which can be safely assumed as the average efficiency of c-Si wafer solar cells at the industrial module level. We report this benchmark value with a dashed white line in Fig. 5. As evident, efficiencies above 20% can be obtained over the entire range of investigated thickness. As it will be explained more in detail in the next results, the thickness range 10-80 µm appears to be the most promising one in order to approach the maximum efficiency. To conclude this section, we want to remark that minority carrier diffusion length has to be above at least 60-70 µm to overcome this 20% threshold. Only c-Si can meet this requirement, since other competing materials such as micro-crystalline and amorphous silicon can hardly achieve L of the order of 10 µm and 500 nm, respectively. This limits the maximum efficiency with ideal light trapping to no more than 15% when using a single p-n junction design.

5 SURFACE RECOMBINATION AND INCREASED SURFACE AREA

The effects of surface recombination in c-Si solar cells with ideal Lambertian light trapping are shown in Fig. 6. Here we assume L_n=20 µm, L_p=200 µm, and we report both the analytic result (top panel), and the numerical ones obtained with Silvaco Atlas (bottom panels).

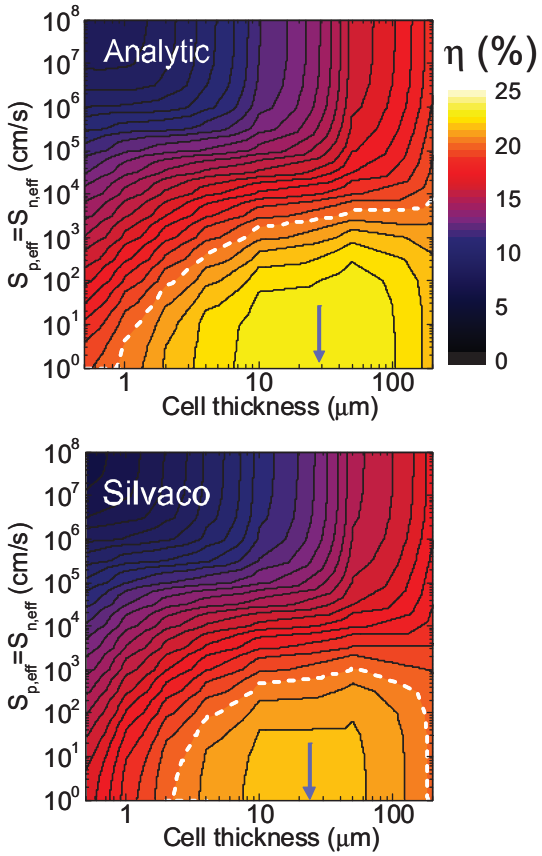

Fig. 6. Effects of surface recombination in c-Si solar cells with ideal Lambertian light trapping and L_p=200 µm, L_n=20 µm. The range for efficiency above 20% is reported within the dashed white line, and the optimal thickness is denoted with a blue arrow.

We note that surface recombination drastically affects the device performance. For S_{eff} below 10^3 cm/s thin film solar cells are more efficient than bulk ones. Above this value, surface losses become dominant, and a bulk design gives better results. We see that if effective surface recombination velocity is kept below 10^2 cm/s, then the cell can be considered as basically free of surface losses, and efficiency approaches the value obtained for perfect passivation (Figs. 3 and 4).

The proposed model is able to reproduce the effects of surface recombination, as it is evident comparing the top and bottom panels of Fig. 6, which refer to analytic and Silvaco ATLAS numerical results. Although the systematic 10% overestimation provided by the model, we see that the trend is reproduced, together with the correct estimation for the optimal thickness.

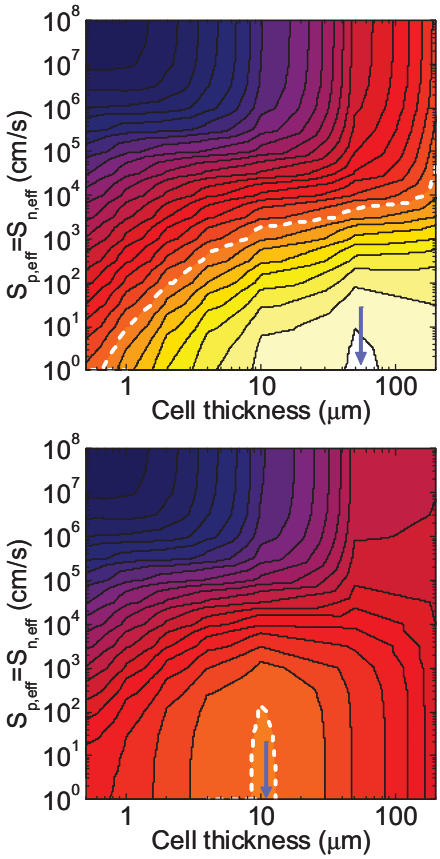

Fig. 7. Effects of surface recombination in c-Si solar cells with ideal Lambertian light trapping and high bulk material quality (L_p=500 µm, L_n=50 µm, top panel), and low quality (L_p=50 µm, L_n=5 µm, top panel). The 20% efficiency and optimal thickness are reported as in Fig. 6. The color scale is the same as in Fig. 6.

To conclude, we compare the effects of surface recombination in solar cells with ideal Lambertian light trapping and different bulk qualities. Analytic results are reported in Fig. 7 for high quality (L_n=50 µm, L_p=500 µm, top panel) and low quality (L_n=5 µm, L_p=50 µm, bottom panel) silicon. We see that higher material quality provides higher efficiency (25%) and larger optimal thickness (60 µm), but always below the limit of 80 µm dictated by intrinsic recombinations. The opposite trend occurs in low quality materials, where thickness around 10 µm gives the best result. In both cases, thin film solar cells with light trapping can be more efficient than bulk ones provided that S_{eff} is kept below 10^3 cm/s. Again,

surface recombination becomes essentially negligible for S_{eff} below 10^2 cm/s.

6 CONCLUSIONS

In conclusion, we developed an analytic electro-optical model for p-n junction c-Si solar cells, and we applied it to investigate the impact of defects-mediated recombinations and light trapping, with special focus on surface recombination. We found that if surface recombination velocities are kept below a critical level which is quantified by the model, then solar cells with thickness in the range 10-80 μm and light trapping are more performing than the bulk ones.
Three main ingredients are needed for these devices to be definitely competitive with textured c-Si wafer solar cells:

- Light trapping at the Lambertian limit;
- Relatively high material quality, comparable with that of bulk wafers (diffusion length larger than a few hundreds of μm);
- Effective surface recombination below 10^2 cm/s.

We note that all these ingredients are achievable with present day's technologies, although they have not yet been implemented together in a single device.
In fact, advanced photonic schemes allows excellent trapping of sunlight not just in bulk wafers [17,22,23], but also in thin films [4-10] down the Wave Optics regime, where thickness is comparable with sunlight wavelengths.
Very good control of the silicon thickness and a bulk material quality comparable or even superior to that of standard c-Si wafers can be obtained using epitaxial layer deposition on a properly prepared silicon substrate. This technique is currently used to produce solar cells with thickness in the range 25-50 μm, with stabilized efficiency in the range 15-19% [13,24]. Recent progress in thin film c-Si processing opens the way to future low cost substrate for high quality epitaxial growth [25,26].
Finally, recalling that $S_{eff} = K_{area}S$, we see that the requirement in terms of surface passivation is achievable. In fact, textures for light trapping that allow approaching the Lambertian limit have characteristic features' sizes comparable with the wavelength of incident sunlight. Very small features and complex morphology are not needed to efficiently trap the light into the silicon layer: the factor K_{area} is thus in the range 1.5 – 2.5 for most of the proposed photonic structures [4,6-10]. State-of-the-art surface passivation techniques allow reducing S down to a few cm/s or even less in silicon, and can be applied successfully also in presence of complex surface morphologies [27,28]. In conclusion, K_{area} around 2.5 and S of the order of 10 cm/s are well compatible with the requirements in terms of S_{eff}.

REFERENCES

1) P. Bermel, C. Luo, L. C. Kimerling, and J. D. Joannopoulos, Opt. Express **15**(25), 16986-17000 (2007).
2) Z. Yu, A. Raman, and S. Fan, Proc. Nat. Acad. Sci. **107**(41), 17941-17496 (2010).
3) J.H. Petermann, D. Zielke, J. Schmidt, F. Haase, E.G. Rojas, and R. Brendel, Progr. Photovolt: Res. Appl. **20**(1), 1-5 (2011).
4) H. Sai, K. Saito, and Michio Kondo, Appl. Phys. Lett. **102**, 053509 (2013).
5) C. Battaglia, C. Hsu, K. Söoderströom, J. Escarré, F. J. Haug, M. Charriére, M. Boccard, M. Despeisse, D. T. L. Alexander, M. Cantoni, Y. Cui, and C. Ballif, ACS Nano **6**(3), 2790-2797 (2012).
6) E.R. Martins, J. Li, Y.K. Liu, J. Zhou, and T.F. Krauss, Phys. Rev. B **86**, 041404(R) (2012).
7) A. Bozzola, M. Liscidini, and L. C. Andreani, Optics Express **20**(S2), A224-A244 (2012).
8) P. Kowalczewski, M. Liscidini, and L.C. Andreani, Opt. Lett. **37**, 4868 (2012).
9) A. Herman, C. Trompoukis, V. Depauw, O. El Daif, and O. Deparis, J. Appl. Phys. **112**, 113107 (2012).
10) K. Vynck, M. Burresi, F. Riboli, and D. S. Wiersma, Nature Materials **11**, 1017-1022 (2012).
11) T. Tiedje, E. Yablonovitch, G. D. Cody, and B. G. Brooks, IEEE transaction on Electron Devices **31**(5), 711-16 (1984).
12) M. A. Green, IEEE transaction on Electron Devices **31**(5), 671-78 (1984).
13) M. A. Green, K. Emery, Y. Hishikawa, W. Warta, and E. D. Dunlop, Progr. Photovolt: Res. Appl. **21**, 1-11 (2013).
14) M. A. Green, Progr. Photovolt: Res. Appl. **7**, 327-330 (1999).
15) M. A. Green, Progr. Photovolt: Res. Appl. **10**, 235-241 (2002).
16) E. D. Palik, Handbook of optical constants of solids (Academic, Orlando 1985).
17) J. Nelson, The Physics of Solar Cells (Imperial College Press, London 2003)
18) R. Brendel, M. Hirsch, R. Plieninger, and J. H. Werner, IEEE Trans. Electon Dev. **43**(7), 1104-1112 (1996).
19) W. J. Yang, Z. Q. Ma, X. Tang, C. B. Feng, W. G. Zhao, and P. P. Shi, Solar Energy **82**, 106-110 (2008).
20) O. Deparis, Opt. Letters **36**(20), 3960-3962 (2011).
21) A. Bozzola, M. Liscidini, and L.C. Andreani, Progr. Photovolt.: Res. Appl. DOI: 10.1002/pip2385 (2013).
22) R.M. Swanson, and R.A. Sinton, Advances in Solar Energy **6**, 427-484 (1990).
23) J. Zhao, A. Wang, M.A. Green, and F. Ferrazza, Appl. Phys. Lett. **73**(14), 1991-1993 (1998).
24) J.H. Petermann, D. Zielke, J. Schmidt, F. Haase, E.G. Rojas, and R. Brendel, Progr. Photovolt: Res. Appl. **20**(1), 1-5 (2011).
25) V. Depauw, Y. Qiu, K. Van Nieuwenhuysen, I. Gordon, and J. Poortmans, Progr. Photovolt: Res. Appl. **19** (7), 844-850 (2011).
26) F. Dross, K. Baert, T. Bearda, et al., Progr. Photovolt: Res. Appl. **20** (6), 770-784 (2012).